# 普鲁士蓝/CdS 纳米复合物电致化学发光及其 $H_2O_2$ 传感应用

史传国[1,2] 徐静娟[1] 陈洪渊*,[1]
([1]南京大学生命分析化学国家重点实验室,南京 210093)
([2]南通大学化学化工学院,南通 226019)

**摘要**: 通过一定体积比的 CdS 和普鲁士蓝(PB)胶体纳米溶液的简单混合,制备了 PB/CdS 纳米复合物。在共反应剂存在条件下,PB 纳米粒子含量较低时,在 ITO 电极上 CdS 纳晶的电致化学发光(ECL)强度可以增强 3 倍左右。PB 纳米粒子含量较高时,CdS 纳晶的 ECL 强度则显著降低。详细讨论了 PB 纳米粒子对 CdS 纳晶 ECL 影响的机理。PB 纳米粒子对 CdS 纳晶的 ECL 增强可用于 $H_2O_2$ 传感。该传感器对 $H_2O_2$ 响应的线性范围为 $3.3\times10^{-8}$~$6.5\times10^{-3}$ mol·L$^{-1}$($R$=0.999 2),检测限为 12 nmol·L$^{-1}$(S/N=3),传感器具有良好的稳定性和重现性。

**关键词**: 普鲁士蓝; CdS 纳晶; 电致化学发光; $H_2O_2$
**中图分类号**: O657.1 **文献标识码**: A **文章编号**: 1001-4861(2011)10-2005-08

# Prussian Blue/CdS Nanocomposite: Enhanced Electrochemiluminescence and Application in $H_2O_2$ Sensing

SHI Chuan-Guo[1,2] XU Jing-Juan[1] CHEN Hong-Yuan*,[1]
([1]*State Key Lab of Analytical Chemistry for Life Science, School of Chemistry and Chemical Engineering, Nanjing University, Nanjing* 210093, *China*)
([2]*College of Chemistry & Chemical Engineering, Nantong University, Nantong, Jiangsu* 226019, *China*)

**Abstract**: Prussian blue (PB)/CdS nanocomposites were prepared under simple ultrasonication mixing of the two separated colloidal solutions at a desired volume ratio. At low amount of PB nanoparticles (NPs), the maximum enhancement factor of about 3-fold in electrochemiluminescence (ECL) intensity of CdS nanocrystals (NCs) was obtained at the indium tin oxide (ITO) electrode in the presence of co-reactant. On the contrary, at high amount PB NPs, the ECL intensity was reduced significantly. The influences of PB NPs to CdS NCs are discussed in detail. The application of the enhanced ECL from the nanocomposite was studied for the $H_2O_2$ sensing. The resulting ECL sensor shows a linear response to the concentration of $H_2O_2$ ranging from $3.3\times10^{-8}$ to $6.5\times10^{-5}$ mol·L$^{-1}$ ($R$=0.9992) with a detection limit of 12 nmol·L$^{-1}$ (S/N=3) and good stability and reproducibility.

**Key words**: prussian blue; CdS nanocrystals; electrochemiluminescence; $H_2O_2$

Electrochemiluminescence, also known as electrogenerated chemiluminescence (ECL), is a means of converting electrical energy into irradiative energy at an electrode. As a valuable detection method, ECL is becoming more recognized in analytical chemistry because of its low background signal, high sensitivity, and simple operation process [1]. Recently, CdS nanocrystals (NCs) has generated enormous interests in ECL analysis due to its easy preparation, wide range of analytes, low oxidation potential, and good chemical stability[2] since Zhu et al.[3] first reported that electrochemical reduced and oxidized CdS NC could

收稿日期:2011-05-24。收修改稿日期:2011-07-08。
国家自然科学基金 (No.20890021),国家 973 计划(No.2007CB936404)资助项目。
*通讯联系人。E-mail:hychen@nju.edu.cn

produce ECL with the coreactant $H_2O_2$. However, compared with traditional luminol and $Ru(bpy)_3^{2+}$ systems, the low ECL signals of CdS NCs restrict its wide analytical applications. Thus, new methods to enhance the intensity of ECL are urgently needed for the development of novel ECL sensors.

To improve the ECL intensity of CdS NCs, nanoparticles (NPs) have been widely used for their unique optical and catalytic properties. Chen et al. [4] have demonstrated that CdS NCs doped with multi-wall carbon nanotubes (MWCNT) show a 5-fold enhanced ECL than CdS NCs film and the ECL starting voltage shifts positively from −1.15 to −0.85 V. Li et al.[5] have indicated that the ECL intensity of CdS-Ag nanocomposite arrays (CdS-Ag NCAs), prepared by 10 min electrodeposition time, is 5-fold of CdS hierarchical nano-arrays (CdS HNAs), and the ECL onset voltage shifts positively by 0.45 V. Xu and co-workers[6] found that the MWCNT-CdS nanocomposite fabricated by an in situ synthesis method showed much more sensitive ECL responses compared with that of the MWCNT/CdS composite obtained under simple ultrasonication mixing at a desired ratio. Wang et al. [7] reported that the presence of the graphene doped in CdS NCs could facilitate the electrochemical redox process of CdS NCs and the as-prepared graphene/CdS nanocomposite could react with $H_2O_2$ to generate strong and stable ECL emission, which not only enhances its ECL intensity by about 4.3-fold but also decreases its onset potential for about 0.32 V. Chen et al. [8] also reported a simple approach to obtain enhanced ECL behavior based on Au/CdS nanocomposite films by adjusting the amount of Au NPs in the nanocomposite. The maximum enhancement factor of about 4 was obtained at an indium tin oxide (ITO) electrode in the presence of co-reactant $H_2O_2$.

Prussian blue (PB) is a long-known functional semiconductor material with photostability, electrocatalytic activity, and ion-exchange properties [9]. Herein, the water soluble PB NPs were prepared and PB/CdS nanocomposites were synthesized by simple mixing of the two separated colloidal solutions by keeping the amount of CdS NCs constant and varying the amount of PB NPs. At low amount of PB, the maximum enhancement factor of about 3-fold in ECL intensity at an ITO electrode in the absence of co-reactant compared with pure CdS NCs were reported. Scanning electron microscope (SEM) and electrochemical impedance spectroscopy (EIS) were conducted to investigate the mechanism of ECL enhancement and quenching. The application of the enhanced ECL from the nanocomposite films was exploited for $H_2O_2$ sensing since a rapid and accurate determination of $H_2O_2$ is of great importance in clinical diagnostics, environmental control, and industry[10].

## 1 Experimental

### 1.1 Chemicals and reagents

Didodecyldimethylammonium bromide (DDAB) was purchased from Sigma. $FeCl_2 \cdot 4H_2O$, $K_3[Fe(CN)_6]$, $CdCl_2 \cdot 2.5H_2O$, $Na_2S \cdot 9H_2O$, thioglycolic acid (TGA), and a 30% $H_2O_2$ solution were purchased from Shanghai Chemical Reagent Company (Shanghai, China). Toluene was purchased from Nanjing Chemical Reagent Company (Nanjing, China). A solution of $H_2O_2$ was freshly prepared before use. 0.1 mol·L$^{-1}$ phosphate buffer solution (PBS) with different pH values was prepared by mixing the stock solutions of $K_2HPO_4$ and $NaH_2PO_4$ and adjusting the pH value with 0.1 mol·L$^{-1}$ $H_3PO_4$ or NaOH solution. All other chemicals were commercially available and of analytical reagent grade, used as received. Water for all solutions was purified using a Milli-Q (Millipore, USA) water purification system.

### 1.2 Preparation of PB NPs

PB NPs were synthesized by modified reported method[11]. DDAB (2.3 g) was first dissolved in 50 mL of toluene. $FeCl_2 \cdot 4H_2O$ (8.9 mg) was added to the DDAB solution. The mixture was sonicated until the entire solid disappeared and a clear yellow reverse-micelle solution was obtained. 450 μL of 0.1 mol·L$^{-1}$ $K_3[Fe(CN)_6]$ solution was slowly added to the reverse-micelle solution at room temperature with vigorous stirring. For the preparation of thiol-capped PB NPs, TGA (20 μL) was added to the resulting micellar solution and the mixture was stirred for 12 h under nitrogen. Pyridine (20 mL) was added to the solution, and the resulting

precipitate was centrifuged and washed with *n*-heptane, petroleum ether, butanol, and ethanol. Then, the TGA-capped PB NPs were obtained after being dried under vacuum. 0.4 mg·mL$^{-1}$ PB stock solutions were obtained via dispersing PB NPs in water under ultrasonication.

### 1.3 Preparation of PB/CdS nanocomposites

The CdS NCs were synthesized according to a method reported earlier[12]. 0.093 g of $CdCl_2 \cdot 2.5H_2O$ was dissolved in 100 mL of water. Then, 0.89 g of TGA as the stabilizer was added to this solution under stirring. The pH value was adjusted to 10 by dropwise addition of 1 mol·L$^{-1}$ NaOH solution. Then, 4.06 mL of 0.5 mol·L$^{-1}$ $Na_2S$ solution was introduced into the system under stirring. The reaction mixture was refluxed for 12 h. Then, ethanol was added with extensive stirring for 10 min, and the yellow precipitate was obtained. The precipitate was collected after centrifuging, subsequently washed three times with anhydrous ethanol, and dried in air. 0.1 mg·mL$^{-1}$ CdS stock solutions were obtained via dispersing CdS NCs in water under ultrasonication.

PB/CdS nanocomposites were synthesized by mixing different volumes of the above PB stock solution and 1 mL of the above CdS stock solution, and then diluted with water to 10 mL under ultrasonication for 30 min. The volume of PB stock solution was 0.001, 0.003, 0.005, 0.01, 0.1 and 0.5 mL, respectively. Therefore, a series of PB/CdS nanocomposite solutions containing an equal amount of CdS NCs and different amounts of PB NPs were obtained. For the convenience of discussion, they are denoted by $PB_{0.001}/CdS_1$, $PB_{0.003}/CdS_1$, $PB_{0.005}/CdS_1$, $PB_{0.01}/CdS_1$, $PB_{0.1}/CdS_1$, and $PB_{0.5}/CdS_1$, respectively. All of the samples were optically clear solution and no precipitate was observed for two months storing at 4 ℃.

### 1.4 Preparation of modified electrodes

The ITO coated glass plates (Southern Glass Holding Company, China) with sheet resistance of ~10 Ω with dimensions of 1.5 cm×1.0 cm were used as electrodes in all experiments. Prior to modification, the ITO electrodes were thoroughly ultrasonic cleaned for 5 min in acetone, ethanol, and water successively, and allowed to dry at room temperature. Then, the above PB/CdS nanocomposite solutions (60 μL) were applied to the ITO electrodes by syringing the solution onto the electrodes. It is important to note that the same amount of composite solutions containing an equal quantity of CdS NCs was deposited on each sample with 1.0 × 1.0 cm$^2$ in size. As a control, pure CdS NCs modified ITO electrodes were also prepared under the same conditions.

### 1.5 Instruments

The transmission electron microscope (TEM) images were recorded using a Tcenai 20 (FEI, USA) TEM. The colloidal solution was dropped on a carbon-coated copper grid, after which the grid was allowed to dry at room temperature before TEM imaging. Ultraviolet and visible (UV-Vis) absorption spectra were recorded with a 3600 UV-Vis-NIR spectrometer (Shimadzu, Japan). Photoluminescence (PL) spectra were obtained on a RF-5301PC spectrofluorometer (Shimadzu, Japan). A Sirion 200 SEM (FEI, USA) was employed to record the images of the nanocomposite films.

The ECL measurements were performed in 0.1 mol·L$^{-1}$ PBS bubbled with $N_2$ for at least 20 min and then a $N_2$ atmosphere was kept over test solution, while electrochemical impedance spectroscopy (EIS) was performed on an Autolab Electrochemical Analyzer (Ecochemie, the Netherlands) in 5.0 mmol·L$^{-1}$ $K_3Fe(CN)_6/K_4Fe(CN)_6$ (1∶1) mixture with 0.10 mol·L$^{-1}$ $KNO_3$ as a supporting electrolyte at its open circuit potential. A conventional three-electrode system was used in the ECL and EIS experiments with a saturated calomel electrode (SCE) as the reference electrode, a Pt wire as the counter electrode, and a PB/CdS nanocomposite film modified ITO electrode as the working electrode. ECL and electrochemical curves were recorded using a Model MPI-A electrochemiluminescence analyzer system (XiAn Remax Electronic Science & Technology Co. Ltd., China). The spectral width of the photo-multiplier tube (PMT) was 200~800 nm.

## 2 Results and discussion

### 2.1 Characterization of PB NPs and CdS NCs

The typical TEM images of TGA-capped PB NPs and TGA-capped CdS NCs are shown in Fig.1a and Fig.

1b. The average diameters of PB NPs and CdS NCs are found to be 20 nm and 3~4 nm, respectively, and their size distributions are narrow.

Although the formation of CdS and PB primarily judged based on the color change of the products, absorption spectra were used to characterize PB NPs and CdS NCs.

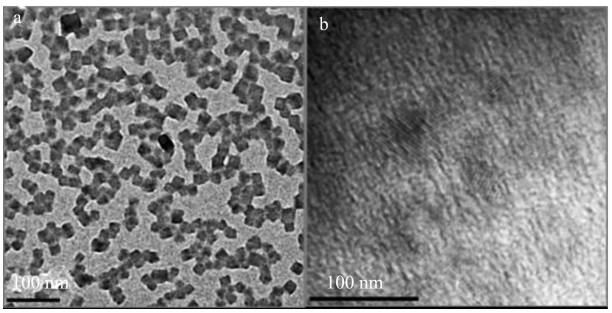


Fig.1 TEM images for PB NPs (a) and CdS NCs (b)

Fig.2a shows the broad band at 700 nm of PB NPs, which is assigned to the intervalence charge-transfer (IVCT (Fe Ⅱ-CN-Fe Ⅲ)) band of PB[11]. In addition, PB NPs bear good electrochemical behaviors. In pH 7.0 PBS, two typical pairs of redox waves showing the oxidation of Prussian Blue to Prussian Green as well as the reduction of Prussian White are observed (inset in Fig.2), which further confirms the synthesis of PB NPs[9]. Fig.2b shows maximum absorption peak at 417 nm of CdS NCs, suggesting the consequence of quantum confinement [13]. The particles size is ~4.0 nm, as calculated in virtue of the empirical equation ($D$=(−6.652 1×10$^{-8}$)$\lambda^3$+(1.955 7×10$^{-4}$)$\lambda^2$−(9.235 2×10$^{-2}$)$\lambda$+13.29, $\lambda$ (nm): the wavelength of the first excitionic absorption peak of the UV-Vis absorption spectrum.) reported previously [14], which is coincidental with the TEM results.

Fig.2c indicates the PL emission peak of CdS NCs colloidal solution at 570 nm ($\lambda_{ex}$=392 nm) known as the characteristic of surface state emissions of NCs.

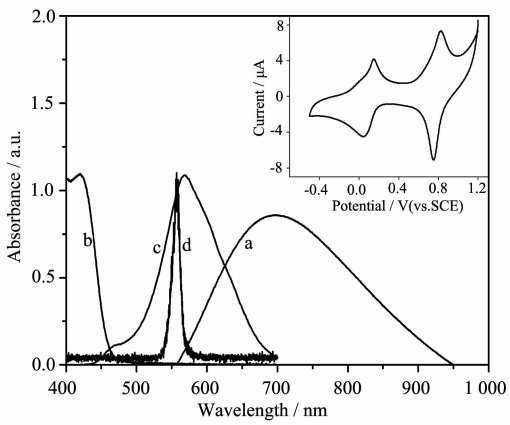


Fig.2 UV-Vis spectrum of PB NPs (a) colloidal solution. UV-Vis spectrum (b) and PL spectrum (c) of CdS NCs colloidal solution. ECL spectrum of CdS NCs (d) at ITO electrode in 0.1 mol·L$^{-1}$ PBS (pH=10) containing 1 mmol·L$^{-1}$ $H_2O_2$ obtained by stepping the potential between 0 and −1.4 V. Inset: Cyclic voltammetric curves (CVs) for the PB NPs modified ITO electrode in 0.1 mol·L$^{-1}$ pH 7.0 PBS in $N_2$ atmosphere at 100 mV·s$^{-1}$

Meanwhile, the observed maximum wavelength of the ECL spectrum at 560 nm is almost equal to the PL emission peak (Fig.2d). This suggests that the ECL emission is also concerning the surface states. ECL is another important tool to study the surface states of NCs. Furthermore, compared with the ECL spectrum of CdS and the absorption spectra of PB, a considerable spectral overlap is not observed. This means that the efficient energy transfer between CdS NCs and PB NPs does not exist[15], which is different from the composites of Au nanoparticles and CdS NCs[8,15].

## 2.2 SEM of PB/CdS nanocomposite films

To assess the morphology of the PB/CdS nanocomposite film, the SEM images of bare glassy carbon (GC) (Fig.3a) and the thin films using 60 μL CdS NCs (Fig.3b), $PB_{0.005}/CdS_1$ (Fig.3c), and $PB_{0.5}/CdS_1$ (Fig.3d) modified GC are shown respectively.

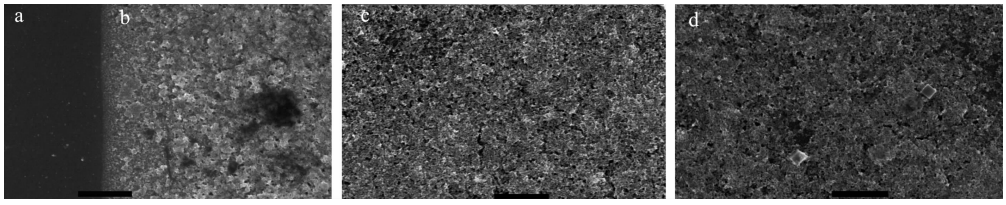


Fig.3 SEM images for a bare GC (a) and CdS NCs (b), $PB_{0.005}/CdS_1$ (c), and $PB_{0.5}/CdS_1$ (d) modified GC with constant amount of CdS NCs. All of the toolbar is 500 nm

At low amount of PB NPs, such as $PB_{0.005}/CdS_1$, relatively homogeneous and close-packed films are formed. At high amount of PB NPs, such as $PB_{0.5}/CdS_1$, some PB NPs can be observed on the interface of the films. The results show that the micrograph of nanocomposite films change with the increasing amount of doping PB NPs.

### 2.3 EIS of nanocomposite films

EIS is an effective tool for studying the interface properties of surface-modified electrodes. The semicircle diameter of EIS equals to the electron transfer resistance ($R_{et}$), which controls the electron transfer kinetics of redox probe ($K_3Fe(CN)_6/K_4Fe(CN)_6$) at electrode surface.

The semicircle diameter of EIS of the bare and NPs modified ITO electrodes increases in the following order: bare ITO electrodes (Fig.4a) <$PB_{0.005}/CdS_1$ modified ITO electrodes (Fig.4c) <CdS NCs modified ITO electrodes (Fig.4b) <$PB_{0.5}/CdS_1$ modified ITO electrodes (Fig.4d). The results reveal that a low amount of PB in the nanocomposite could accelerate electron transfer process occurring on the surface of the modified electrode [16] and a high amount of PB NPs in the composite could obstruct electron transfer process due to its poor conductivity as a common semiconductor. Thus, PB NPs could significantly influence the electron-transfer resistance of the composite films.

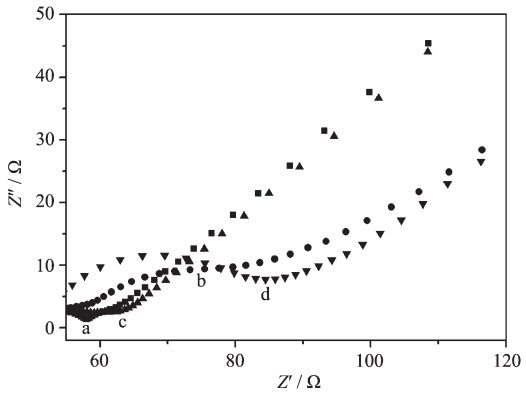


Fig.4 EIS of bare ITO electrode (a), and CdS NCs (b), $PB_{0.005}/CdS_1$ (c), and $PB_{0.5}/CdS_1$ (d) modified ITO electrodes

### 2.4 ECL behaviors of PB/CdS nanocomposite films

According to previous reports [17], the reduced species of CdS NCs ($CdS^-$) can react with the coreactants, such as $H_2O_2$, to produce excited states ($CdS^*$) which generate ECL in the aqueous system. Fig.5 corresponds to the ECL-potential curves for the pure CdS NCs (a) film and $PB_{0.005}/CdS_1$ nanocomposite (b) film in 0.1 mol·$L^{-1}$ PBS (pH=10) containing 10 μmol·$L^{-1}$ $H_2O_2$.

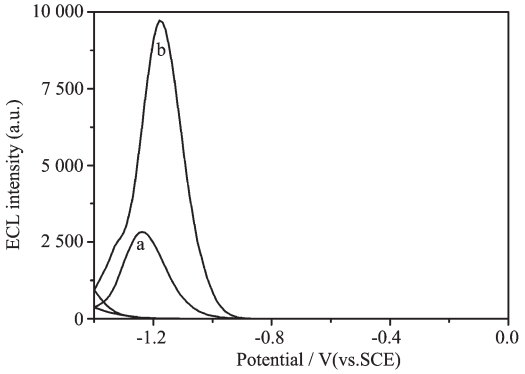


Fig.5 ECL intensity versus potential on CdS NCs (a) and $PB_{0.005}/CdS_1$ (b) modified ITO electrodes in 0.1 mol·$L^{-1}$ pH 10 PBS containing 10 μmol·$L^{-1}$ $H_2O_2$ in $N_2$ atmosphere at 100 mV·$s^{-1}$. The voltage of the PMT was set at 800 V

The maximum ECL signal appears at about −1.2 V as the potential is scanned in the negative direction from 0 to −1.4 V at 100 mV·$s^{-1}$. In this case, CdS NCs are firstly reduced to $CdS^{-\cdot}$ by charge injection, then $CdS^{-\cdot}$ reacts with $H_2O_2$ to produce $CdS^*$, which decays to the ground state with light emitting. However, it is highlighted that the ECL intensity of $PB_{0.005}/CdS_1$ nanocomposite film is ca. 3-fold higher than that of pure CdS NCs film. Moreover, there is no ECL signal for bare ITO electrode and PB NPs modified ITO electrode under the same conditions. Therefore, the ECL signal is from the CdS NCs and could be enhanced by compositon with PB NPs.

Since PB NPs doping could significantly affect the ECL behaviors of CdS NCs, the effect of the amount of PB NPs in the composite on the ECL response was studied. As shown in Fig.6, the ECL intensity increases as the amount of PB NPs increases. The highest ECL intensity is obtained at $PB_{0.005}/CdS_1$ modified ITO electrodes. PB NPs show the catalytic properties to the reduction of $H_2O_2$[9], however, the amount of PB NPs in nanocomposites is relatively low and when

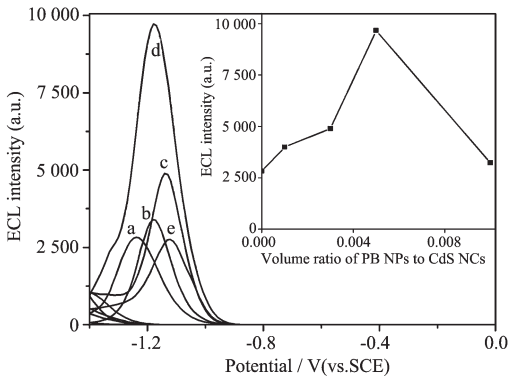


Fig.6 ECL intensity profiles for pure CdS NCs (a) and the PB/CdS nanocomposite films with different amount of PB NPs, such as, $PB_{0.001}/CdS_1$ (b), $PB_{0.003}/CdS_1$ (c), $PB_{0.005}/CdS_1$ (d), and $PB_{0.01}/CdS_1$ (e) modified ITO electrodes in 0.1 mol·L$^{-1}$ pH 10 PBS containing 10 μmol·L$^{-1}$ $H_2O_2$ in $N_2$ atmosphere at 100 mV·s$^{-1}$. The voltage of the PMT was set at 800 V. Inset: plot of volume ratio of PB NPs to CdS NCs versus the ECL intensity

nanocomposite immobilizes on electrodes, the two typical pairs of redox waves of PB NPs and the catalytic behavior to the reduction of $H_2O_2$ could not be observed (not shown).

Thus, the enhancement of ECL is possibly attributed to the smaller resistance of the composite film as EIS experiment shows, which increases the reaction rate and leads to the formation of more $CdS^*$ in the film. However, as the amount of PB NPs further increases, the ECL response decreases rapidly. It is reasonable that when more PB NPs are doped in CdS NCs, the impedance of the modified electrodes surface is increased because of the poor conductivity of PB NPs as a common semiconductor, which is also confirmed by the results of EIS. And the possible ECL enhancement and quenching mechanism of PB/CdS nanocomposites are different from that of Au/CdS[8] and MWCNT/CdS[4] nanocomposites. According to the experimental results, the strongest ECL is obtained at $PB_{0.005}/CdS_1$ modified electrodes. Therefore, $PB_{0.005}/CdS_1$ as an optimum amount of PB NPs was used in all the subsequent experiments.

## 2.5 Sensing application of PB/CdS nanocomposite

At $PB_{0.005}/CdS_1$ modified ITO electrode, the ECL intensity in 0.1 mol·L$^{-1}$ pH 10 PBS after air saturated was obtained. When dissolved oxygen was removed from the solution by bubbling $N_2$ for 20 min, ECL intensity decreased dramatically. Thus, dissolved oxygen participated in the ECL light emission process. In order to improving the accurateness, $N_2$ atmosphere was used in all ECL process. The amount of PB/CdS nanocomposite used in fabrication process of the modified electrodes strongly affects the ECL behaviors which are very sensitive to the surface properties and dependent on the surface state. The effect of volume of $PB_{0.005}/CdS_1$ colloidal solution for nanocomposite film modified ITO electrode on ECL intensity was also examined. It is found that the ECL intensity, which is related to the production of $CdS^-$, increases with the volume of $PB_{0.005}/CdS_1$ colloidal solution for deposition up to 60 μL (not shown). The further increase in the volume of composite for modified electrodes might lead to the increase of the impedance of the electrode and the change of the surface state of the films. Therefore, the optimum volume of 60 μL of composite was used in all experiments.

$H_2O_2$ could obviously enhance the ECL intensity after bubbling with $N_2$ for 20 min. Thus, the $PB_{0.005}/CdS_1$ modified ITO electrode could be used to develop an ECL sensor for the detection of $H_2O_2$ in aqueous solution. Under optimized fabrication conditions, the effect of pH value for the electrolyte solution on the ECL behaviors was examined. With an increase in solution pH value from 5 to 11, the ECL intensity of the $PB_{0.005}/CdS_1$ in the presence of 10 μmol·L$^{-1}$ $H_2O_2$ increases greatly and then tends to a constant value at pH value of 10 (not shown). The enhancement in ECL emission in the presence of $H_2O_2$ is mainly due to the adsorption of Lewis bases, which change the surface states of composite film[18]. Considering the analytical performance of the ECL sensor, pH value of 10 was chosen for determination procedure.

Controlling the ECL properties of NCs by $H_2O_2$ might provide a new and versatile method to develop NCs-based sensors. Fig.7 shows the sensing response of $PB_{0.005}/CdS_1$ nanocomposite modified ITO electrode to $H_2O_2$ under the optimum conditions. A linear relation

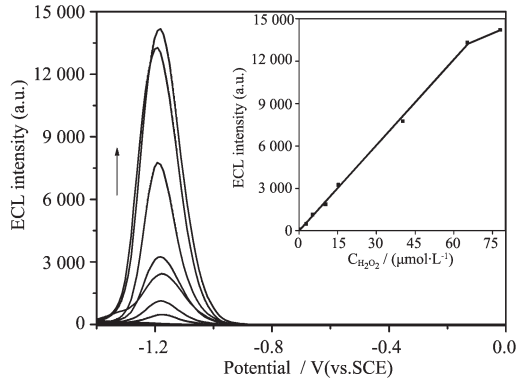


Inset: calibration curve for $H_2O_2$ detection. The voltage of the PMT was set at 400 V

Fig.7　Effect of $H_2O_2$ concentration on ECL intensity of $PB_{0.005}/CdS_1$ thin film modified ITO electrode in 0.1 mol·L$^{-1}$ PBS (pH=10) containing 2.5, 5.0, 10.0, 15.0, 40.0, 65.0, and 78.0 μmol·L$^{-1}$ $H_2O_2$ (from lower to upper) at 100 mV·s$^{-1}$

between the ECL intensity and $H_2O_2$ concentration is obtained from $3.3\times10^{-8}$ to $6.5\times10^{-5}$ mol·L$^{-1}$ with a correlation coefficient of 0.9992 ($n$=8). The detection limit is 12 nmol·L$^{-1}$ at a signal-to-noise ratio of 3.

As summarized in Table 1, the present ECL $H_2O_2$ sensors based on $PB_{0.005}/CdS_1$ nanocomposite films exhibit wider linear dynamic range and lower detection limit than those of the other ECL $H_2O_2$ sensors based on CdSe film[19], CdS hollow spheres thin film[20], and CdS nanotube [21]. And, the detection performance of ECL sensor for $H_2O_2$ based on $PB_{0.005}/CdS_1$ film at the present stage is as efficient as that of the ECL system based on luminol-enzyme composite[22].

The present ECL sensor showed good reproducibility. The fabrication of three sensors showed an acceptable reproducibility with a relative standard deviation of 3.3% at 10 μmol·L$^{-1}$ $H_2O_2$ level. Fig.8 shows the ECL emission from the $PB_{0.005}/CdS_1$ films under continuous potential scanning for 20 cycles. Stable and high ECL signal are observed, which suggests that the sensor is suitable for ECL detection. After this electrode was stored under dark conditions for one month, the ECL response did not show an obvious decline, demonstrating good stability.

**Table 1　Performance comparison of the $H_2O_2$ ECL sensors based on different materials depositing on the electrodes**

| Material | Linear range / (μmol·L$^{-1}$) | Detection limit / (μmol·L$^{-1}$) | Reference |
|---|---|---|---|
| CdS bollow spheres | 0.12~8.7 | 80 | 20 |
| CdS nanotubes | 0.5~10.0 | 100 | 21 |
| CdSe NCs | 0.25~10.0 | 100 | 19 |
| PB/CdS NCs | 0.03~78.0 | 12 | This study |

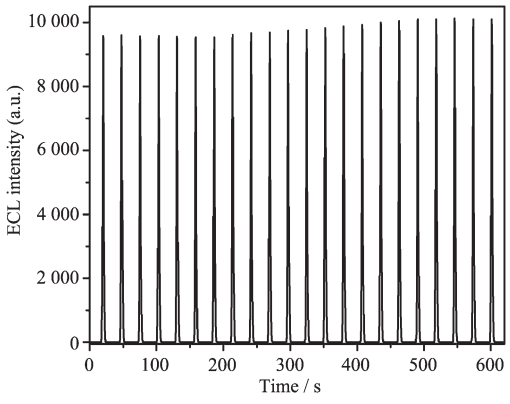


The voltage of the PMT is set at 800 V

Fig.8　ECL emission from $PB_{0.005}/CdS_1$ modified ITO electrodes in 0.1 mol·L$^{-1}$ PBS containing 10 μmol·L$^{-1}$ $H_2O_2$ under continuous CVs between 0 and −1.4 V for 20 cycles at 100 mV·s$^{-1}$

## 3　Conclusions

In summary, enhanced ECL responses were obtained using PB/CdS nanocomposite thin film deposited on ITO electrode surface in aqueous solutions. Under optimal conditions, the ECL intensity of $PB_{0.005}/CdS_1$ nanocomposite films is ca. 3-fold higher than that of pure CdS NCs films. The interesting enhancement would be useful for analysis and detection based on ECL methods of PB/CdS nanocomposite. Such an ECL $H_2O_2$ sensor has much better response than that from the other NPs with good stability, sensitivity, and reproducibility.

**References**:

[1] Richer M M. *Chem. Rev*., **2004**,**104**:3003-3036

[2] Burda C X, Chen R, Narayanan M.A, et al. *Chem. Rev*., **2005**,**105**:1025-1102

[3] Ren T, Xu J Z, Tu Y F, et al. *Electrochem. Commun*., **2005**,**7**:5-9

[4] Ding S N, Xu J J, Chen H Y. *Chem. Commun*., **2006**,**36**: 3631-3633

[5] Wang C Z, E Y F, Fan L Z, et al. *J. Mater. Chem*., **2009**,**19**: 3841-3846

[6] Wang X F, Zhou Y, Xu J J, et al. *Adv. Funct. Mater*., **2009**,**19**:1-7

[7] Wang K, Liu Q, Wu X Y, et al. *Talanta*, **2010**,**82**:372-376

[8] Shi C G, Xu J J, Chen H Y. *Electrochimica Acta*, **2010**,**27**: 8268-8272

[9] Zhao G, Feng J J, Zhang Q L, et al. *Chem. Mater*., **2005**,**17**: 3154-3159

[10]Wang C L, Mulchandani A. *Anal. Chem*., **1995**,**67**:1109-1114

[11]Taguchi M, Yagi I, Nakagawa M, et al. *J. Am. Chem. Soc*., **2006**,**128**:10978-10982

[12]Spanhel L, Haase M, Weller H, et al. *J. Am. Chem. Soc*., **1987**,**109**:5649-5655

[13]Ludolph B, Malik M A, OBrien P, et al. *Chem. Commun*., **1998**,**20**:1849-1850

[14]Yu W W, Qu L, Guo W, Peng X G. *Chem. Mater*., **2003**,**14**: 2854-3860

[15]Shan Y, Xu J J, Chen H Y. *Chem. Comm*., **2009**, 905-907

[16]Zhao W, Xu J J, Shi C G, et al. *Langmuir*, **2005**,**21**:9630-9634

[17]Haram S K, Quinn B M, Bard A J. *J. Am. Chem. Soc*., **2001**, **123**:8860-8861

[18]Brainard R J, Ellis A B. *J. Phys. Chem. B*, **1997**,**101**:2533-2539

[19]Zou G G, Ju H X. *Anal. Chem*., **2004**,**76**:6871-6876

[20]Dai Z, Zhang J, Bao J, et al. *J. Mater. Chem*., **2007**,**17**: 1087-1093

[21]Jie G, Liu B, Miao J, et al. *Talanta*, **2007**,**71**:1476-1480

[22]Fahnrich K A, Pravda M, Guibault G G. *Talanta*, **2001**, **54**:531-559